The energy dependence of the phase shifts can be "explained" in terms of simple static potentials. There definitely appears to be a resonance in the state of isotopic and ordinary spin both $\frac{3}{2}$, and the resonant energy occurs near $\eta=1.67$, corresponding to an energy of 200 Mev. No states of higher angular momenta are required up to and including data at 217 Mev, if the Fermi solutions are assumed to be correct.

The low-energy behavior of the S-wave phase shifts may be completely different than described. The low-energy data are still too poor to permit us to say definitely that α_3 changes sign. It is seen in Fig. 5 that the given models predict a dip in the total positive pion-proton cross section in the region from 10 to 30 Mev. It would be difficult to distinguish this from an energy dependence for α_3 in which α_3 remains negative but levels off. However, such a dependence would not give a rise below 10 Mev, and very low-energy total cross sections would be valuable in determining the low-energy behavior of α_3.

At this point it is appropriate to express our indebtedness to the members of the meson scattering group for their assistance and the use of their electronics equipment.

We wish to thank Dr. Jay Orear, Dr. Lederman, Dr. Homa, and Dr. Noyes for sending reprints and for very helpful communications. Professor Gregory Breit contributed a valuable discussion of effective-range theory.

We wish to thank Mrs. R. Cutosky, Mrs. F. Feiner, Mr. J. Morrison, Mr. R. Klein, Mr. G. Stranahan, and Miss J. Kugell for their efficient scanning.

PHYSICAL REVIEW VOLUME 97, NUMBER 3 FEBRUARY 1, 1955

π^--p Interactions at 1.4 Bev*

L. M. Eisberg, W. B. Fowler, R. M. Lea,† W. D. Shephard,‡ R. P. Shutt, A. M. Thorndike, and W. L. Whittemore
Brookhaven National Laboratory, Upton, New York

(Received October 6, 1954)

π^--p interactions have been observed in the hydrogen filling of diffusion cloud chambers exposed to a π^- beam of average energy 1.37 Bev at the Brookhaven Cosmotron. If 9 interactions leading to heavy unstable particles are omitted, there remain 147 interactions observed with magnetic field and 323 interactions without field. The total cross section is estimated to be 34.6±2.7 millibarns. The elastic scattering cross section is 10.0±0.8 millibarns. The elastic scattering angles are mostly less than 60° in the center-of-mass system and are accordingly interpreted as mainly due to diffraction scattering. The observations are consistent with diffraction by a sphere with radius $(1.18\pm0.10)\times10^{-13}$ cm and transparency 0.61±0.10. However, the 20 percent of elastic scattering observed through angles >60° may indicate a region of very strong interaction with radius $\sim0.5\times10^{-13}$ cm surrounded by a region of much weaker interaction. Of the inelastic events only the 95 observed in the magnet cloud chamber can be analyzed further. Of these 71 to 81 are considered to involve the production of one secondary pion and 14 to 24 two pions, depending on the assignment of unidentified inelastic cases. This indicates a slightly greater multiplicity than predicted by Fermi's statistical theory. Angle and momentum distributions of emitted pions are discussed in terms of possible pion-pion interactions and excited nucleon states, but conclusions on these questions are uncertain.

THIS paper reports some results concerning the nature of π^--p collisions at an energy of about 1.4 Bev. It is the second dealing with a preliminary cloud chamber survey of nucleon-nucleon and pion-nucleon interactions at the Cosmotron, the previous one having been concerned with n-p collisions at about 1.7 Bev.[1] The paper on n-p collisions will be referred to as I.

A considerable number of investigations of pion-nucleon interactions have been made at energies up to about 250 Mev,[2] but higher energy experiments have until recently been possible only with cosmic rays, and there are few cases where pions could be identified and their behavior studied.[3] A number of measurements of π-p total cross sections have been made using pion beams at the Cosmotron,[4] and π-p interactions have been studied in nuclear emulsions exposed to a 1.5-Bev π^- beam.[5]

In this experiment π-p interactions are observed in the hydrogen gas filling of diffusion cloud chambers, which are operated in a negative pion beam with average energy 1.37 Bev. (The experimental procedure is described in Sec. II.) Consequently, there is little ambiguity concerning the nature of the interacting particles. The situation is more definite than was the

* Work performed under the auspices of the U. S. Atomic Energy Commission.

† Now at Yale University, New Haven, Connecticut.

‡ Now at University of Wisconsin, Madison, Wisconsin.

[1] Fowler, Shutt, Thorndike, and Whittemore, Phys. Rev. **95**, 1026 (1954), henceforth referred to as I.

[2] For summary see Henley, Ruderman, and Steinberger, Ann. Rev. Nuc. Sci. **3**, 1 (1953).

[3] See, for example: Camerini, Fowler, Lock, and Muirhead, Phil. Mag. **41**, 413 (1950); R. L. Cool and O. Piccioni, Phys. Rev. **87**, 531 (1952).

[4] Shapiro, Leavitt, and Chen, Phys. Rev. **92**, 1073 (1953); S. J. Lindenbaum and L. C. L. Yuan, Phys. Rev. **92**, 1578 (1953); Cool, Madansky, and Piccioni, Phys. Rev. **93**, 249 (1954); **93**, 637 (1954).

[5] Crussard, Walker, and Koshiba, Phys. Rev. **94**, 736 (1954); Walker, Crussard, and Koshiba, Phys. Rev. **95**, 852 (1954).

case in I because the π^- beam has a more definite energy than the neutron beam, and the tracks of incident particles are seen. Elastic π^--p scatterings are easily found, while elastic n-p scatterings were not often recorded and were, therefore, ignored in I. One might expect that the theoretical interpretation of π-p interactions would be somewhat simpler than that of n-p interactions, since only one nucleon is present.

I. OBJECTIVES OF THE EXPERIMENT

The experiment described here was intended to give a qualitative picture of the nature of π^--p interactions and, if possible, to provide information on the following specific questions:

1. Production of "new unstable particles." Cosmic ray observations had suggested that many instances of production of heavy unstable particles were due to pions, and it was of interest to attempt to confirm this observation. A few examples of production of such particles in π^--p collisions have been reported in detail.[6] Several more will be discussed in a later paper. This paper will discuss the other π^--p interactions observed.

2. Multiplicity of pion production. As in I, it is of interest to determine the number of cases in which 0, 1, 2, · · · secondary pions are produced in addition to the incoming pion. It was shown in I that two pions are frequently produced in n-p collisions, but there was some indication that one pion may have been emitted from each nucleon involved in the collision. In π^--p collisions only one nucleon is present, so that a comparison of the two results should provide information concerning the mechanism of pion production.

3. Angular distribution of elastic scattering. It should be of interest to compare the angular distribution with that observed at lower energies. In particular, the existence of inelastic interactions should lead to elastic diffraction scattering which would have a characteristic forward angular distribution. Such an effect could, in principle, yield information concerning the size and opacity of a proton.

4. Energy, angle, and charge of emitted particles. In addition to pion multiplicity such detailed information is of interest for comparison with theories of pion production.

5. Angular correlations between emitted particles. Such angular correlations may give evidence of meson-nucleon or meson-meson forces acting between emitted particles. If the forces are strong enough to produce definite intermediate states (as, for example, an excited nucleon with spin and isotopic spin$=\frac{3}{2}$) this condition should be recognized.

II. EXPERIMENTAL PROCEDURE

The observations were made with two diffusion cloud chambers filled with hydrogen at a pressure of about 20 atmospheres, with methyl alcohol as condensable vapor. One group of photographs was taken in a 16-inch diameter chamber provided with a magnetic field of about 10 500 gauss, and a second group was taken in a chamber 6 feet long and 11 inches wide with no magnetic field. The procedure is similar to that followed in I. Details of the cloud chambers have been described.[7]

The π^- beam was selected by a channel about $2\frac{1}{2}$ inches high and 10 inches wide in the Cosmotron shield, placed so that negative pions emitted in a forward direction from the target in the straight section were deflected through the channel by the magnetic field in the following quadrant of the Cosmotron. The channel was one similar to that used by Cool, Madansky, and Piccioni[4] except that the width was greater. 2.2-Bev circulating protons struck a carbon target at a radius of 350 inches. After emerging from the Cosmotron shield the beam was bent through about 16° by an analyzing magnet and allowed to pass through a channel in the 3-foot wall of a concrete block house around the cloud chamber.

Under these conditions the beam has an average momentum of 1.50 Bev/c (kinetic energy 1.37 Bev) as determined by measurements of the momentum of a group of beam tracks in the magnet cloud chamber. These measurements were made by projecting through a prism following Blackett's procedure.[8] The system was calibrated with photographs of ruled curves of known curvature. The momentum spectrum is shown in Fig. 1. The width of the main group is partly due to errors in measurement. Pion trajectories were plotted to determine the expected beam momentum, with results entirely consistent with the cloud chamber

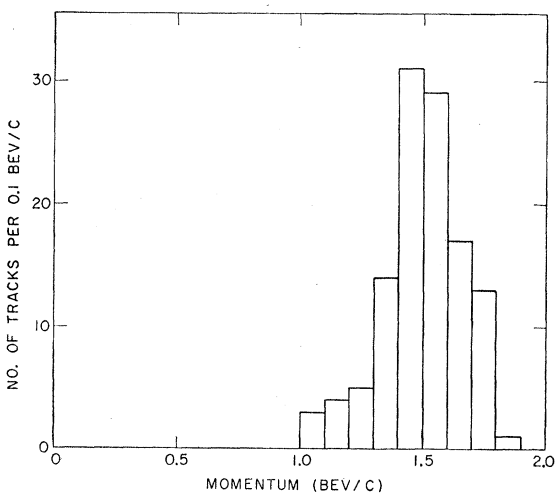

FIG. 1. Momentum spectrum of π^- beam determined from momentum measurements on 117 beam tracks in the magnet cloud chamber.

[6] Fowler, Shutt, Thorndike, and Whittemore, Phys. Rev. **91**, 1287 (1953); **93**, 861 (1954).

[7] Fowler, Shutt, Thorndike, and Whittemore, Rev. Sci. Instr. **25**, 996 (1954).

[8] P. M. S. Blackett, Proc. Roy. Soc. (London) **A159**, 1 (1937).

TABLE I. Types of π^--p interactions considered in this article.

Type	Charge state[a]	Number of secondary pions	Number of prongs	Number of neutral particles
Elastic	$(p-)$	0	2	0
Inelastic (recorded)	$(p-0)$	1	2	1
	$(n+-)$	1	2	1
	$(p-00)$	2	2	2
	$(n+-0)$	2	2	2
	$(p-+-)$	2	4	0
Charge exchange and inelastic (not recorded)	$(n0)$	0	0	2
	$(n00)$	1	0	3
	$(n000)$	2	0	4

[a] For example, $(n+-)$ means that neutron, π^+, and π^- result from the collision.

value, when energy loss in passing through the Cosmotron wall was taken into account. Since the channel is fairly wide, the plotted trajectories also indicate a momentum spread of about ± 0.1 Bev/c. The low-energy tail presumably results from pions that scatter from the channel walls or have unusually large energy loss in passing through the wall of the Cosmotron vacuum chamber. The *average* momentum of 1.50 Bev/c has an uncertainty of about ± 0.05 Bev/c. The "beam" contains tracks within an angular spread of ± 5 degrees for the magnet chamber, and $\pm 4°$ for the long chamber. Tracks outside this range were omitted in all instances.

About 28 000 Cosmotron pulses were photographed with the magnet chamber and about 14 000 with the 6-foot chamber. The pictures were scanned for deflections or interactions of beam tracks. Disappearances-in-flight were occasionally noted, but no attempt was made to scan for them, since in scanning it was difficult to distinguish them from tracks leaving the sensitive region or entering gaps, and since their interpretation would be ambiguous in any case (see Table I). Angles were measured in space relative to the incoming pion direction, using projectors that reproduced the geometry of the cameras. Curvatures were measured with a micrometer stage microscope. Momenta are corrected, when appropriate, for optical distortion, magnification, and for velocity parallel to the magnetic field, but the measurements are not accurate enough to justify detailed corrections for conical projection.

If one assumes that the frequency of events with the production of three or more secondary mesons is negligible, the events to be expected are as listed in Table I. Events resulting in heavy unstable particles are omitted.

The $(p-+-)$ events are easily recognizable because they are the only type with four emerging prongs. The elastic events can be identified by the fact that emergent tracks are coplanar, and angles and momenta have the values required to conserve energy and momentum.

The identification of the inelastic $(p-0)$, $(n+-)$, $(p-00)$, and $(n+-0)$ events is more difficult, however, since they all involve two prongs whose energy and momentum fail to balance because of the presence of one or more neutral particles. There is no practical means of distinguishing between these possibilities unless there is a magnetic field so that momenta can be measured. In principle measurement of the momentum and density of ionization of the positive tracks would determine which were protons and which pions, while conservation of momentum and energy would determine unambiguously whether one or more neutral particles were involved. In practice our measurements are not usually accurate enough to do so, and some element of uncertainty is present as to the classification of the events. The details of the procedure used in classifying them are given in Sec. V.

III. TOTAL CROSS SECTION

This experiment provides a direct measurement of the total cross section from the number of scattering events observed and the pion path length. The best way to determine the total pion path length is by counting π-μ decays, as was done at lower energies.[9] The largest possible deflection resulting from π-μ decay for a 1.4-Bev π meson is 1.54°. This angle is too small to be discovered with any degree of certainty in the magnet chamber photographs. The photographs of the long cloud chamber, however, were scanned with a distorted projected image which magnified small angles by a factor of about five, and π-μ decays could be observed easily. Consequently the path length for data taken with the long chamber could be determined by the π-μ count, while it was necessary to count beam tracks in the magnet chamber photographs. The two estimates are, therefore, discussed separately.

With the magnet chamber corrections are necessary for beam contamination, inefficiency in scanning, and interactions having all neutral prongs, which were not recorded. To obtain an accurate total cross section, it is necessary to determine the corrections for these effects carefully. We have only made rough estimates of these corrections, so that the resulting value for the total cross section is correspondingly approximate.

The length of beam tracks in the magnet chamber pictures was measured in every 50th picture in every other 100-foot roll of film, counting all tracks that had entry angle within $\pm 5°$ of the average beam direction, and momentum that was not obviously incompatible with 1.50 Bev/c. From the average track length per picture and total number of pictures taken, the total track length was estimated to be 17 000 g/cm^2 of H_2. The muon contamination is probably higher than the 5.4 percent determined by Cool, Madansky, and Piccioni[4] because of the wider channel, and a few low energy tracks probably were included. An estimate of (15 ± 10) percent seems reasonable for the beam contamination as the beam was defined here.

[9] Fowler, Fowler, Shutt, Thorndike, and Whittemore, Phys. Rev. **91**, 135 (1953).

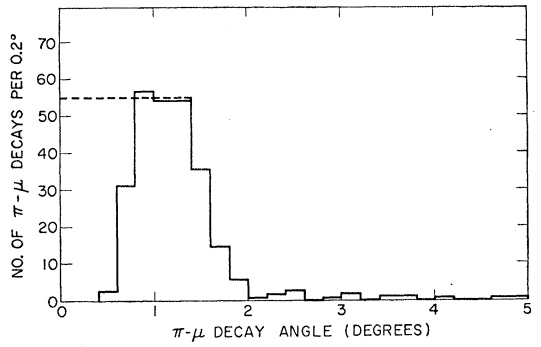

FIG. 2. Distribution of projected angles of π-μ decay deflections. A cut-off angle of 1.54° corresponds to a pion energy of 1.4 Bev. The dashed line represents an extrapolation to zero angle.

The actual number of interactions observed was 151, (including 4 events resulting in heavy unstable particles which must be included in the total cross section). The number of unrecorded zero prong events (resulting in neutral particles only) was estimated as 22, as described in Sec. IV, leading to a total of 173 interactions. The scanning procedure was certainly not 100 percent efficient. In fact, a "fast scanning" procedure was used for most of the magnet chamber pictures, which involved only area scanning and no repeated scanning. Consequently, there was no experimental determination of the efficiency. On the basis of previous experience it seems appropriate to assume an efficiency of (80±10) percent under these circumstances. With all these corrections taken into account, the cross section obtained is 25±6 millibarns.

A more reliable value is found with the long chamber. Here it has been possible to determine the intensity of the incident pions directly by counting the number of π-μ decays observed.[9] In this manner the effect of beam contamination is eliminated. Also the scanning efficiency is of little importance since it has been determined that in general the chances for missing π-μ decays and scattering events are about equal.

A total of 532 π-μ events were observed. Their distorted *projected* angles were converted to actual values. The distribution of projected π-μ decay deflections is shown in Fig. 2. Ideally this distribution should be constant and be cut off sharply at the largest possible π-μ decay angle. Actually the distribution appears to be flat only between 0.8° and 1.4°. Above 1.4° it falls off fairly rapidly to a negligibly small value at 1.8°. Cut-off angles between 1.4° and 1.8° correspond to a pion momentum spectrum between 1.7 and 1.3 Bev/c, respectively, in agreement with the magnetically measured spectrum given in Fig. 1. Deflections below 0.8° were often missed as seen in Fig. 2. A correction is made by extending the distribution to zero angle as indicated by the dashed line in Fig. 2. The integral under the distribution represents the total number of π-μ decays that should have occurred inside the chamber and gives a value of 903±50 cases. As previously[9] the lifetime of the pions is taken to be 2.55×10^{-8} sec.

The absolute hydrogen pressure was 21.3 atmos, and the average temperature −40°C. A total of 323 π^--p collisions with two or four emitted prongs were found in the hydrogen. From the given data a cross section of 32.4±2.3 millibarns would follow. However, closer inspection of the ratio of the number of interactions to the number of π-μ decays in different locations in the chamber shows that near the ends of the chamber too few π-μ decays were found since there either the incident π or the outgoing μ track became so short that the relatively small deflections could not be observed reliably. Omitting all events occurring in the regions near the ends, one is left with 452 π-μ decays and 250 interactions. These values lead to a more reliable cross section of 29.7±2.4 millibarns. Adding 5 events showing production of heavy unstable particles not yet included results in a cross section of 30.3±2.5 millibarns. To obtain the total cross section we have again the estimated correction, amounting to 14.6 percent, for the zero-prong events which were not recorded. (See Sec. IV). The final value for the total π^--p cross section at 1.4 Bev is 34.6±2.7 millibarns, in good agreement with the value of 34±3 millibarns obtained by counter methods.[4] We feel that the magnet chamber result of 25±6 millibarns involves no real discrepancy in view of the uncertainties in the correction factors. (Actually the counter value was obtained at a slightly higher pion energy than that of our beam, but probably the π^--p cross section varies very slowly in this energy region.)

Conversely, one might conclude that the difference between the counter value of 34±3 mb and our value of 30.3±2.5 mb is due to the reactions resulting in neutral particles only, such as charge exchange, (n0), and the inelastic reactions (n00) and (n000). The cross section for these reactions is then 3.7±3.7 mb, which is quite small compared to the value of 30.3 mb for reactions resulting in charged prongs. This is quite different from the observations on π^--p collisions at lower energies (<200 Mev) where up to twice as much charge exchange scattering as ordinary scattering has been observed.

IV. ELASTIC EVENTS

It is often difficult to be sure to which one of the inelastic classes a particular event belongs, even when observed in the magnet chamber, but the criteria described in Sec. II usually make it fairly clear whether an event is elastic or inelastic. Any event for which the observations were consistent, within errors, with the specifications of an elastic event was classified as "elastic."[10] The remainder were considered to be inelastic. They are discussed in Sec. V.

[10] In many cases, of course, the errors of measurement were great enough that one could also devise an inelastic event that would fit them. It seems unlikely, however, that inelastic events

With this procedure 52 events were classed as elastic and 95 as inelastic in the magnet chamber, or 35.4 percent were elastic. The distribution of the angles through which pions were scattered in the elastic events is given in Table II, columns 1 and 2. Here ΔN is the number of angles observed in the angular interval $\Delta\theta$ in the laboratory system. The majority of the elastic scatterings are at angles less than 30°, which implies that the differential cross section is very strongly peaked in the forward direction.

In the long chamber 110 events were classed as elastic and 213 as inelastic. Thus 34.0 percent were elastic, in agreement with the magnet chamber data. The distribution of the scattering angles from the 110 elastic events is given in Table II, columns 3 and 4. Comparison of columns 2 and 4 shows that the distributions for the two chambers agree within the statistical uncertainties. We shall, therefore, lump the data together for the further discussion of the elastic events.

Both distributions lack events with scattering angles $<5°$. Few are expected because of the small available solid angle. A reasonable distribution should result in ≥ 9 percent scattering into angles $\leq 5°$. Instead we find zero percent for the magnet chamber, and 4 ± 2 percent with the long chamber. An interference effect due to Coulomb scattering is not an explanation for the discrepancy since at the present high energies Coulomb scattering becomes important only at scattering angles $<1°$. The discrepancy might be entirely due to statistical fluctuations. In addition, in the magnet chamber, where "area scanning" only was employed, a small deflection might be missed even though a heavily ionized recoil proton should emerge at the point of deflection, since a short proton track might not make itself too apparent among heavily ionized background tracks. In the long chamber a few small angle scatterings may have been counted as π-μ decays.

TABLE II. Distribution ($\Delta N/\Delta\theta$) of elastic scattering angles in the laboratory system.

	(1)	(2)	(3)	(4)
$\Delta\theta$	Magnet chamber		Long chamber	
(Degrees)	ΔN	%	ΔN	%
0–5	0	0	4	4±2
5–10	12	23±7	32	29±5
10–15	15	29±7	25	23±5
15–20	8	15±5	15	14±4
20–25	6	11±5	6	5±2
25–30	2	4±3	3	3±2
30–60	4	8±4	7	6±2
60–90	3	6±3	7	6±2
90–120	2	4±3	8	7±2
120–150	0	0	2	2±2
150–180	0	0	1	1±1
Total	52	100	110	100

would often disguise themselves as elastic ones in view of all the other possibilities at their disposal. Thus any event which could be elastic is considered actually to be elastic, so that one obtains an upper limit for the number of elastic scatterings, but this upper limit is probably close to the true number.

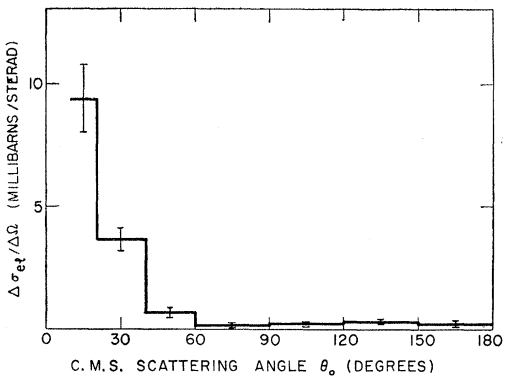

FIG. 3. Center-of-mass angular distribution of all elastic scattering events from magnet and long chambers. Data from the interval $\theta_0 = 0-10°$ are omitted.

We shall make use only of the data for angles $\geq 5°$ in the laboratory system. The combined elastic scattering distribution $\Delta\sigma_{el}/\Delta\cos\theta_0$ in the c.m. system is given in Fig. 3.

Since there are a large number of inelastic events and the elastic scatterings are largely confined to forward angles, it seems natural to conclude that the elastic scattering is largely a diffraction scattering effect, which is a consequence of the inelastic scattering. Such diffraction scattering is a necessary consequence of the inelastic interactions.[11] If there is a "reaction" cross section for an incoming wave of certain angular momentum, then a partial cross section for diffraction scattering for that angular momentum follows from quantum mechanics.

The role of diffraction scattering is clear if one considers pion-nucleon collisions to occur in a way similar to that involved in Fermi's statistical theory of meson production. There is assumed to be a region of strong interaction about the nucleon with radius of about 10^{-13} cm. Since $\lambda\!\!\!^{-}_0$ (in c.m. system) for the pion is about 2.7×10^{-14} cm, we may consider it either to hit this region and interact or miss it and fail to do so. If it hits, the region may then emit two or more pions, in which case the process is obviously a "reaction," or it may re-emit one pion as an elastic scattering. In the latter case the event should be counted as a "reaction" if the emitted pion is considered to arise from a truly "thermal" process so that its phase is random with respect to the incoming pion and cannot interfere with it (incoherent elastic scattering). In this case any pion which hits the strongly interacting region undergoes a "reaction" and there should be an equal number of elastic diffraction scatterings.

If, however, the events in which a single elastic pion is emitted from the region of interaction are considered to arise from "potential scattering," they should not be counted as "reactions," but one should

[11] See, for example, J. M. Blatt and V. F. Weisskopf, *Theoretical Nuclear Physics* (John Wiley and Sons, Inc., New York, 1952), Chap. VIII.

then consider the interference of such outgoing waves with those arising from diffraction scattering. The picture becomes more complicated for such coherent elastic scattering.

It is clear that some distinction should be made between elastic diffraction scattering and the elastic scatterings predicted in the statistical theory. It seems reasonable to interpret the forward peak of Fig. 3 as diffraction scattering (up to $\sim 60°$ in c.m. system), while the large angle elastic events are thought to arise through the statistical process. One interesting qualitative observation can now be made: that the number of elastic cases is considerably less than the number of inelastic ones, and therefore, the region in which the interaction is so strong as to establish thermal equilibrium is rather transparent to the incident pions, a situation which seems inconsistent.

To make the situation more specific we will develop a phenomenological picture of a proton as a partially transparent sphere using the methods commonly applied to nuclei.[12] If we assume that the sphere is a purely absorbing one (resulting in incoherent reactions only), we can determine the size of the sphere from the reaction cross section σ_a, and diffraction cross section σ_d, using Bethe and Wilson's curve for $k_1\lambda=0$. (Here k_1 depends on the size of the potential, if one is present, and λ is the mean free path in nuclear matter, assumed to be zero in the "thermal" picture.)

We have observed a total of 33 scatterings through c.m. system angles greater than 60° which should be counted toward σ_a following the "thermal" model. Since in the purely statistical model the angular distribution for incoherent scattering is assumed to be isotropic, a statement with which Fig. 3 is not inconsistent, we will add 11 more events from the $\theta_0=0$ to 60° interval, giving 44 incoherent scatterings. (Solid angle for $\theta_0=0$ to 60° is $\frac{1}{4}$ of solid angle for $\theta_0=0$ to 180°.) There were also the 9 events resulting in production of heavy unstable particles.[6] In addition, an allowance must be made for unrecorded events ($n0$), ($n00$), and ($n000$). An estimate was made using statistical weights calculated by Fermi[13] and the observed numbers of inelastic events resulting in charged particles from Part V, leading to 70 unobserved events.[14] The total number of diffraction scatterings is then $162-44=118\pm15$, and the total number of reactions is $308+44+9+70=431\pm20$. If we now divide the total cross section of 34 millibarns in this proportion, we obtain $\sigma_a=26.7\pm1.3$ millibarns, $\sigma_d=7.3\pm1.0$ millibarns. These values are consistent[12] with a radius, $R=(1.18\pm0.10)\times10^{-13}$ cm, and transparency $=\sigma_a/\pi R^2=0.61\pm0.10$. One can make a rough estimate of the angular distribution expected by using the Bessel function formula[12] applicable to an opaque sphere. Taking $R=1.18\times10^{-13}$, one obtains the expected distribution given by the curve in Fig. 4. A better estimate might be obtained by treating the proton as a transparent sphere, in which a pion mean free path of $\lambda=1.5\times10^{-13}$ cm corresponds to the observed transparency. Using the methods of Fernbach, Serber, and Taylor[12] one obtains a distribution that differs very little from that for the opaque sphere. The observed diffraction scattering distribution also given in Fig. 4 seems to be somewhat weighted toward larger angles, but the discrepancy hardly seems significant.

Perhaps the most important experimental deviation from the "thermal" model, postulating a sphere of radius R with very strong interaction, lies in the fact that the amount of diffraction scattering is less than $\frac{1}{3}$ the amount of incoherent interaction. An alternate treatment might be to interpret *all* of the observed elastic scattering as due to coherent scattering from

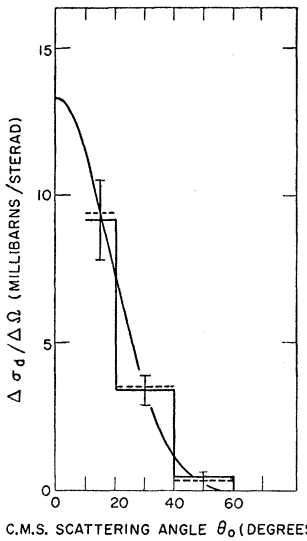

FIG. 4. Center-of-mass distribution of elastic scattering events considered to be due to diffraction scattering. Here all large-angle scattering events have been treated as incoherent. The dashed lines give the average values of the theoretical curve, corresponding to the intervals used for plotting the experimental data. The derived radius of interaction of $R=1.18\times10^{-13}$ cm was used.

[12] Fernbach, Serber, and Taylor, Phys. Rev. **75**, 1352 (1949); H. A. Bethe and R. R. Wilson, Phys. Rev. **83**, 690 (1951).

[13] E. Fermi (private communication).

[14] These weights were calculated making use of the hypothesis of charge independence. Within each state of multiplicity the probabilities for the different reactions are then given. (See Table I.) A π^--p collision can proceed through the isotropic spin $T=\frac{1}{2}$ or $\frac{3}{2}$ state. In Fermi's statistical calculation the results from these two states were mixed in the ratio 2:1, respectively. If only elastic and charge exchange scattering occurred, the correction for ($n0$) would depend very strongly on whether or not the reaction really proceeds according to this ratio, since for $T=\frac{1}{2}$ twice as much elastic as charge exchange scattering is expected while this ratio is reversed for $T=\frac{3}{2}$. Since, however, mostly single meson production is observed (Sec. V), the correction should mostly take into account the reaction ($n00$), which amounts to 17 percent of all single meson production for $T=\frac{1}{2}$, to 13 percent for $T=\frac{3}{2}$, and to 16 percent for the mixture used by Fermi. Thus the correction of 70 for the unobserved events should not depend much on the initial isotopic spin state. That a correction of this magnitude really applies has also been shown in Sec. IV, where its application brought about agreement between cloud chamber and counter values. (The excited nucleon model also leads to corrections of the given magnitude.)

a sphere within which the interaction varies from very strong near the center to rather weak at the outside. The observed scattering through large angles ($\theta_0=60°$ to 180°) would then be due to interactions occurring near the center (s- and perhaps p-waves, $L=0$, 1), while most of the observed forward scattering would come from the outer regions ($L=2$, 3, 4). For instance, a calculation shows that making the mean free path in nuclear matter $\lambda\approx 0$ for $L=0$, 1, and $\lambda\approx 5\times 10^{-13}$ cm for $L=2$, 3, 4 (up to a radius $R=1.4\times 10^{-13}$ cm) would result in the observed cross section $\sigma_{el}=10$ millibarns, $\sigma_{inel}(=34-\sigma_{el})=24$ millibarns, and would also give a large angle tail similar to the observed one. Of course, instead of a step function for λ, some continuous function can also be used to give a similar result. Such a function might, for instance, be similar to the Yukawa potential which indeed gives an average interaction ~ 20 times stronger in the region $L=0$, 1 than in the region $L=2$, 3, 4. If "potential scattering" were admitted we would have to use complex phase shifts instead of the purely imaginary ones used so far, and other possibilities exist to fit the observed data. One such possibility is to assume $\lambda\approx 4\times 10^{-13}$ cm = constant in a sphere with radius $R=1.4\times 10^{-13}$ cm and to have a potential well with depth ~ 500 Mev in the region $L=0$, 1.[15] Very probably, however, such an elementary picture is much oversimplified, particularly in the light of the known difficulties at relativistic energies. Nevertheless, the fact remains that all of the experimental data can be accounted for by the assumption of a very strongly interacting region with average radius $\sim 5\times 10^{-14}$ cm and a surrounding much more weakly interacting region up to $R\approx 1.4\times 10^{-13}$ cm.

V. PION MULTIPLICITIES AND CHARGE STATES

Of the charge states listed in Table I, the $(p-)$ and $(p-+-)$ are definitely identified as described in Sec. II. With the long chamber no further distinction can be made. With the magnet chamber pictures one can classify inelastic events as $(p-0)$ or $(n+-)$, $(p-00)$ or $(n+-0)$, but the problem is more difficult, and it is necessary to follow a procedure somewhat like that used in I for the classification of n-p interactions. In the π^- case, however, the incident energy is known, which makes the analysis of cases with one outgoing neutral particle somewhat more definite, and makes it possible to try to determine whether two outgoing neutral particles are involved. The following discussion refers only to magnet chamber events, except where noted explicitly.

In analyzing the events the first problem is to try to identify the positive track as a π^+ or proton. All events were analyzed on this basis, without considering identification as a K^+ a possibility, since there should be few K^+ particles. In some cases the positive track could be identified by density of ionization and momentum. In some additional cases tracks at angles greater than 75° could be identified as π^+ since protons cannot be emitted at such large angles from inelastic events.[16] In addition, a proton emitted at an angle close to the maximum must be denser than minimum, so the limiting angle can be made a few degrees smaller for minimum tracks.

If the positive track is identified as a proton and both momenta are measured, then the mass of a single neutral particle can be calculated, in principle, by:

$$M_4=(E_4^2-p_4^2)^{\frac{1}{2}}, \tag{1}$$

$$E_4=E_1+M-E_2-E_3, \tag{2}$$

$$\mathbf{p}_4=\mathbf{p}_1-\mathbf{p}_2-\mathbf{p}_3. \tag{3}$$

Here E_1, p_1 are total energy and momentum of the incident π^-, E_2, p_2; E_3, p_3 are total energy and momentum of the two outgoing tracks; E_4, p_4 are those of the neutral particle. M is mass of struck proton. If one obtains $M_4=0.14$ Bev, or can obtain such a result by adjusting p_2, p_3, and the angles of these tracks within their experimental errors, the event is classed as $(p-0)$. If, however, one cannot select values within the experimental errors that give $M_4=0.14$, but only higher values of M_4, the event must be classed as $(p-00)$. (The two π^0's carry off more total energy than corresponds to their resultant momentum, and so, in general, would be expected to appear like a single particle of higher mass.) If either $M_4=0.14$ or $M_4=0.28$ was possible within the errors of measurement on 2 and 3, the event was classed as $(p-0)$ because it is unlikely that there would really be two π^0's going with the same velocity in so nearly the same direction that their total energy and momentum would closely resemble a single π^0. If, however, either p_2 or p_3 is measured poorly, it may not be possible to determine whether the event is $(p-0)$ or $(p-00)$. Each event must be considered as an individual case.

If the positive track is identified as a proton, and only one outgoing momentum measured, say p_2, then various choices of p_3 are tried. In each case p_4 is then determined by Eq. (3), and assuming the event is $(p-0)$, $E_4=(p_4^2+0.14^2)^{\frac{1}{2}}$. If this value of E_4 satisfies Eq. (2) within ± 0.05 Bev, that value of p_3 is considered to give a satisfactory solution as a $(p-0)$ event. If $E_1+M>E_2+E_3+E_4$, an additional π^0 is required. In most cases values of p_3 could be chosen appropriate to either $(p-0)$ or $(p-00)$ classifications.

If the positive track is identified as a π^+, the corresponding calculations are made to test whether the event should be classified as $(n+-)$ or $(n+-0)$.

If the positive track is not identified, and one or

[15] There are several theoretical mechanisms to produce such large forces of very short range. Short-range forces have been treated by R. Jastrow [Phys. Rev, **81**. 165 (1951)] and related to pion field theory by M. M. Lévy [Phys. Rev. **88**, 725 (1952)] and S. D. Drell and E. M. Henley [Phys. Rev. **88**, 1053 (1952)]. Other suggestions involve heavy particles, such as K-mesons, etc.

[16] R. M. Sternheimer, Phys. Rev. **93**, 642 (1954).

TABLE III. Classification of inelastic events.

$(p-0)$	16
$(p-00)$	1
$(p-0)$ or $(p-00)$	6
$(n+-)$	8
$(n+-0)$	6
$(n+-)$ or $(n+-0)$	23
$(p-+-)$	4
"unidentified inelastic"	31
Total	95

both momenta are measured, all four possibilities must be considered and an attempt made to see whether any of them is more or less consistent with the observations than the others.

If the positive track is not identified and neither momentum measured, the event is simply classed as "unidentified inelastic" and no calculations made.

Table III shows a breakdown of inelastic events. The "unidentified inelastic" category includes all those which could be classified in either of two or more classes except for the possibilities "$(p-0)$ or $(p-00)$" and "$(n+-)$ or $(n+-0)$" which are tabulated explicitly. For example, an event which could be $(p-0)$ or $(n+-)$ or $(n+-0)$ would simply be tabulated as "unidentified inelastic."

There are certainly some cases in which two secondary pions are produced, a total of 11 being listed. The number classified as single secondary pion cases is 24, the number that are uncertain is 60. Under these conditions one cannot say much concerning the frequency of double pion production.[17] If one simply apportions the uncertain cases in the same ratio as the classified ones, i.e., $24/7=[(p-0)+(n+-)]/[(p-00)+(n+-0)]$, one obtains totals of 71 single pion cases and 24 double pions. On the other hand the most reliable double pion cases are the $(p-+-)$, which are rare. If one makes the $(p-+-):(p-00):(n+-0)$ ratio fit the Fermi statistical weights[18] of 1.4:1:2.3 one would infer that since only $4(p-+-)$ were observed, there should be about $3(p-00)$ and $7(n+-0)$, with the remaining 81 cases all single pion production.[18]

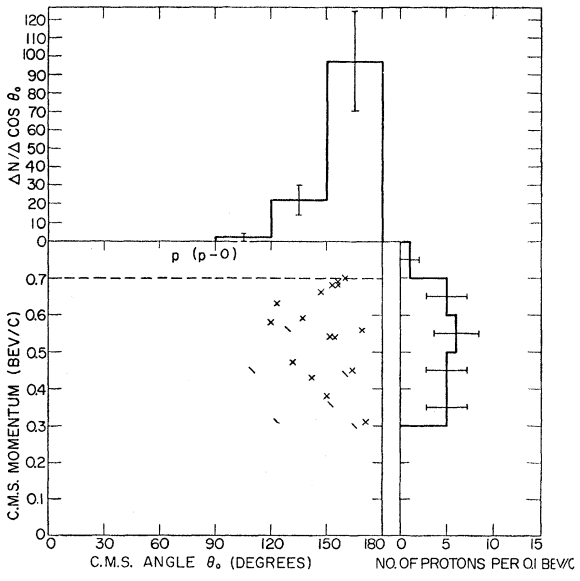

FIG. 5. Center-of-mass scatter diagram of the protons from the reaction $(p-0)$. At the top the differential angular distribution of the protons is plotted, and at the right their momentum distribution. The dashed line in the scatter diagram shows the maximum c.m. system momentum for protons. Events identified as probable $(p-0)$ are plotted as oblique crosses (×). Events identified as $(p-0)$ or $(p-00)$ are plotted as oblique lines (\), using angles and momenta that fit the $(p-0)$ possibility.

These numbers should be compared with the frequency of zero pion production cases, leaving out those due to diffraction scattering, that is, to the large-angle elastic scatterings, of which there were 9 with $\theta_0>60°$, or 12, correcting for those with $\theta_0<60°$, assuming isotropic distribution. This is done in Table IV, for the usual nucleon radius of $R=1.4\times10^{-13}$ cm and also for the $R=1.18\times10^{-13}$ cm derived in Sec. IV, which is more consistent with this experiment. The figures given for the statistical theory are based on an approximation in which pions are taken to be extremely relativistic, and it is probable that more exact calculations such as those of Yang and Christian[19] would favor lower multiplicities. The discrepancy between observation and statistical theory does not seem to be as striking as in I, however.

TABLE IV. Number of cases with different pion multiplicities.

No. of pions	Uncertain inelastic divided proportionately	Division based on No. of $(p-+-)$	Statistical theory $R=1.4$ $\times10^{-13}$ cm	Statistical theory $R=1.18$ $\times10^{-13}$ cm
0[a]	12	12	22	34
1	71	81	65	61
2	24	14	20	12

[a] Omitting diffraction scattering cases.

The division between $(p-0)$ and $(n+-)$ events is also of interest. Using the Fermi statistical weights the ratio $(p-0)/(n+-)$ is 17/21, but if it is assumed that the reaction goes through an intermediate excited state with $T=\frac{3}{2}$ the ratio is decreased to 37/76. Using the estimate of 3 $(p-00)$ and 7 $(n+-0)$ one gets correspondingly 20 $(p-0)$ and 30 $(n+-)$, with ratio 0.67, which could be consistent with either predicted ratio, so no decision is possible. The predicted ratio $(p-+-):(p-00):(n+-0)$ for the reaction going

[17] The reason why it is harder to determine the double to single ratio here than in I is that in the events studied in I the single pion cases had no neutral particles emerging, the double pion cases one neutral. Here one must distinguish between one neutral and two neutrals, which is much harder.

[18] In the long chamber 6 $(p-+-)$ events were observed in the total of 323 events. This would correspond to ~3 events in the present 147 obtained with the magnet chamber, in agreement with the four actually found.

[19] C. N. Yang and R. S. Christian, Brookhaven internal report (unpublished).

through an intermediate $T=\frac{3}{2}$ state is 78:55:115 which is not appreciably different from that based on Fermi's statistical weights, so the double meson production cases could not be used to decide this question.

VI. DISTRIBUTIONS OF ANGLES AND MOMENTA OF INELASTIC EVENTS

The angular distribution of elastic scatterings has been discussed in Sec. IV. We now consider the angles and momenta of the particles emitted in inelastic events. Unfortunately, there are not very many events which provide useful information, since momentum measurements on the "unidentified inelastic" are incomplete or nonexistent. Furthermore, whenever there are two neutral particles, as in $(p-00)$ or $(n+-0)$, the angles and momenta of the neutral particles cannot be

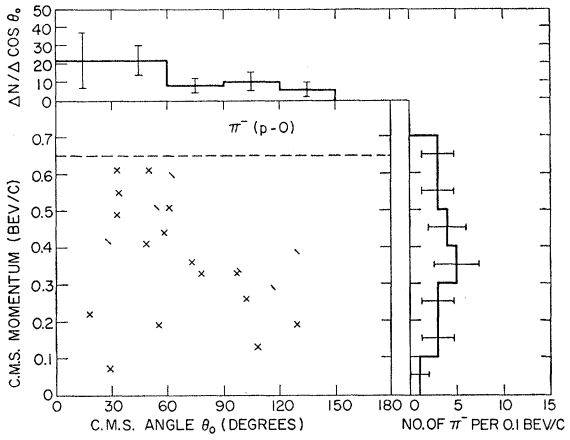

FIG. 6. Center-of-mass scatter diagram of the π^- from the reaction $(p-0)$. At the top the differential angular distribution of the π^- is plotted, and at the right their momentum distribution. The dashed line in the scatter diagram shows the maximum c.m. system momentum for π^-. Events identified as probable $(p-0)$ are plotted as oblique crosses (×). Events identified as $(p-0)$ or $(p-00)$ are plotted as oblique lines (\), using angles and momenta that fit the $(p-0)$ possibility.

determined unambiguously from energy and momentum balance. As a result it does not seem worth while to analyze distributions of angles and momenta except for $(p-0)$ and $(n+-)$ events.

There is still an element of uncertainty in the events classed as "$(p-0)$ or $(p-00)$" and "$(n+-)$ or $(n+-0)$" in Table III. According to the discussion presented in Sec. V it is probably most reasonable to think that most of these events are $(p-0)$ or $(n+-)$ respectively, since the number of $(p-+-)$ events is small. We have included all "$(p-0)$ or $(p-00)$" events as $(p-0)$ in the angle and momentum distributions, and all "$(n+-)$ or $(n+-0)$" as $(n+-)$, since it is not possible to tell which of them should be excluded. The same procedure was followed by Crussard, Walker, and Koshiba in analyzing events found in emulsions.[5] One should remember, however, that a few cases of mistaken identity are, no doubt, included.

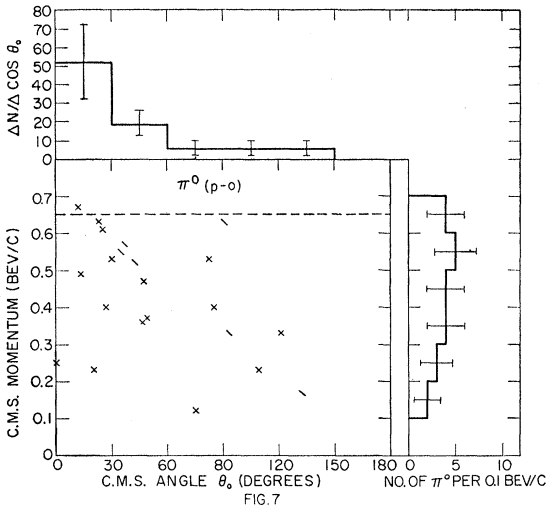

FIG. 7. Center-of-mass scatter diagram of the π^0 from the reaction $(p-0)$. At the top the differential angular distribution of the π^0 is plotted, and at the right their momentum distribution. The dashed line in the scatter diagram shows the maximum c.m. system momentum for π^0. Events identified as probable $(p-0)$ are plotted as oblique crosses (×). Events identified as $(p-0)$ or $(p-00)$ are plotted as oblique lines (\), using angles and momenta that fit the $(p-0)$ possibility.

The data are summarized by the scatter diagrams shown in Figs. 5–10 which plot momentum *vs* angle in the center-of-mass system. In analyzing these data one must note that the selection of events has introduced a bias in favor of events in which the positive particle goes backwards in the center-of-mass system. If the positive particle (p or π^+) goes forward in the c.m.

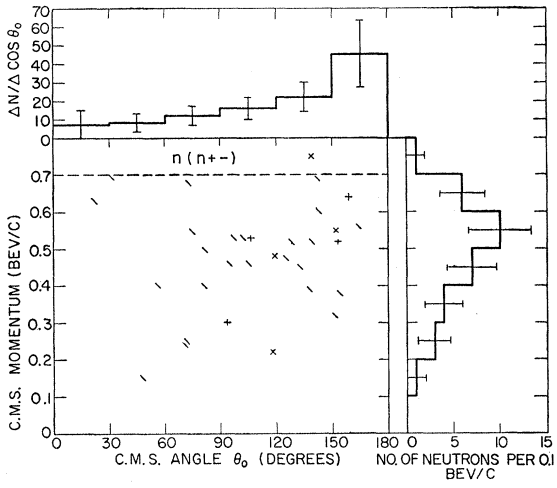

FIG. 8. Center-of-mass scatter diagram of the neutrons from the reaction $(n+-)$. At the top the differential angular distribution of the neutrons is plotted, and at the right their momentum distribution. The dashed line in the scatter diagram shows the maximum c.m. system momentum for the neutrons. Events identified as definite $(n+-)$ are plotted as vertical crosses (+), those identified as probable $(n+-)$ as oblique crosses (×). Events identified as $(n+-)$ or $(n+-0)$ are plotted as oblique lines (\), using angles and momenta that fit the $(n+-)$ possibility.

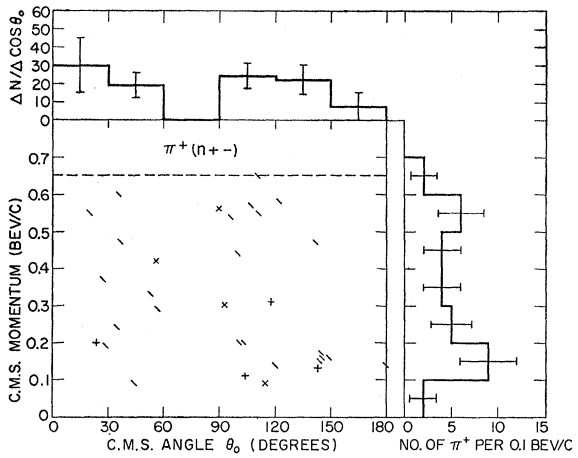

FIG. 9. Center-of-mass scatter diagram of the π^+ from the reaction $(n+-)$. At the top the differential angular distribution of the π^+ is plotted, and at the right their momentum distribution. The dashed line in the scatter diagram shows the maximum c.m. system momentum for the π^+. Events identified as definite $(n+-)$ are plotted as vertical crosses (+), those identified as probable $(n+-)$ as oblique crosses (×). Events identified as $(n+-)$ or $(n+-0)$ are plotted as oblique lines (\) using angles and momenta that fit the $(n+-)$ possibility.

system, its laboratory momentum is usually so high that it is not possible to tell whether it is p or π^+. Such events are classed as "unidentified inelastic" and not included. This bias probably accounts for the backwards preference of the $\pi^+(n+-)$[20] and to some extent for the sharp backwards peak for $p(p-0)$.

Even allowing for this bias, however, it seems that the angular distributions show a backward preference for the nucleons and a forward preference for the pions, as shown in Fig. 11. The momentum distribution of the nucleons is peaked at high momenta, while that for the pions is much broader, as shown in Fig. 12.

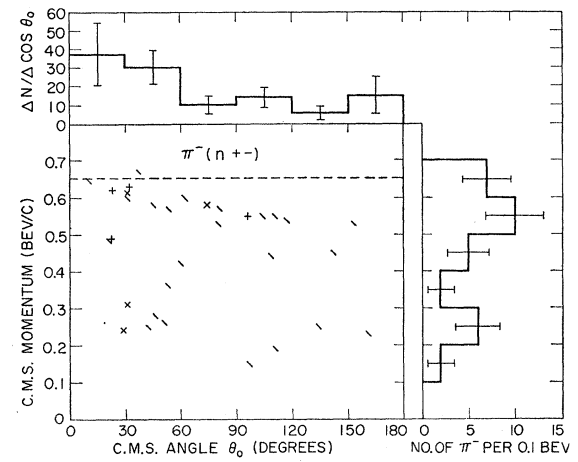

FIG. 10. Center-of-mass scatter diagram of the π^- from the reaction $(n+-)$. At the top the differential angular distribution of the π^- is plotted, and at the right their momentum distribution. The dashed line in the scatter diagram shows the maximum c.m. system momentum for the π^-. Events identified as definite $(n+-)$ are plotted as vertical crosses (+), those identified as probable $(n+-)$ as oblique crosses (×). Events identified as $(n+-)$ or $(n+-0)$ are plotted as oblique lines (\) using angles and momenta that fit the $(n+-)$ possibility.

[20] The symbol $\pi^+(n+-)$ means π^+ mesons from $(n+-)$ events, and similarly for $n(n+-)$, etc.

These results can be discussed from two points of view, which are not necessarily mutually exclusive. From the diffraction scattering interpretation of the elastic events one concludes that the region in which the incident pion interacts has a radius of about 1×10^{-13} cm. This region contains the nucleon and virtual pions making up its pion field in some strongly interacting association. The forward angular preference of the pions and backward preference of the nucleons would be expected if the incoming pion collides with a virtual pion in some cases, rather than with the nucleon itself, so that momentum transfer to the nucleon would be small. On the other hand the pion momentum spectrum resembles what would be expected if the low momentum pions were emitted by a $T=J=\frac{3}{2}$ state with excitation ~160 Mev as was already suggested by the results in I.

A simple way to check whether the data are consistent with the idea of π-π collisions is to calculate the angle between the two outgoing pions. For a collision between an incoming pion of 1.37 Bev and a stationary pion this angle varies from 45° to 90° in the laboratory system. Of course, the virtual pion would be expected often to have a momentum of at least $\mu c=0.14$ Bev/c which would modify the angles considerably. Kovacs has calculated the distribution of the angle between the two pions using scalar theory and obtained a curve peaked strongly at 0° for strong pion-pion interaction.[21] The experimental results are given in Table V. There is indeed a preference for angles of 45°–90°. The forward peak is not marked, but there is a greater preference for forward angles than indicated by Kovacs' curve for strong pion-nucleon interaction. Of course calculations based on scalar theory may not be a reliable guide to the interpretation of the experimental results, but the results are not inconsistent with the possibility that meson-meson interactions play a significant role.

TABLE V. Angle between emitted mesons in laboratory system.

Angle θ_{12}	Number of cases (+−) from $(n+-)$	(−0) from $(p-0)$	Total	Kovacs prediction π-π	π-p
0–60	7	11	18	35	19
60–90	16	9	25	15	14
90–120	8	2	10	3	11
120–150	1	0	1	1	10

If, on the other hand, one expects the interaction to lead to an excited state of the nucleon which then decays to emit the pion with lower c.m. system momentum, this fact should show up most clearly in the momentum spectrum. In addition one should be able to calculate Q values for the excited state. If we take

[21] J. S. Kovacs, Phys. Rev. 93, 252 (1954).

0.16 Bev for the excitation energy, the c.m. system momentum of the scattered pion is 0.55 Bev/c, while that for the pion emitted from the excited nucleon is spread about a most probable value of about 0.3 Bev/c. The pion momentum distribution in Fig. 12 fits this prediction very well. The low-momentum hump on this curve is probably to some extent due to the bias favoring low-energy π^+, however, so this agreement may be fortuitous.

The best evidence for an excited state might be obtained by calculating Q values for nucleon-pion pairs. In particular, the pair $(n-)$ which involves a pure $T=\frac{3}{2}$ state should give Q values near 0.16 Bev. The distribution of Q values is given in Table VI. One would expect low Q values for the pion emitted from the excited state, high apparent Q values (to conserve energy and momentum) for the scattered pion. There is some indication of such a grouping in the $(n+-)$ events, but since the $(n+)$ pair has the most definite low Q value group it may well be a spurious effect due to the bias favoring low energy positive particles. While the data certainly do not prove the existence of an excited state, they are not in disagreement with such a picture either.

TABLE VI. Q values for different pion-nucleon pairs.

Q value Bev	Number of cases From $(p-0)$ $(p-)$	$(p0)$	From $(n+-)$ $(n+)$	$(n-)$
0–0.1	3	2	9	3
0.1–0.2	3	3	8	5
0.2–0.3	5	3	2	1
0.3–0.4	2	3	1	5
0.4–0.5	3	3	1	3
0.5–0.6	5	3	9	7
0.6–0.7	1	5	1	6
>0.7	0	0	0	1

It may seem confusing that the results at the same time show some properties of strong pion-pion interactions and of strong pion-nucleon interactions, but this probably involves no real inconsistency. One can imagine that the incoming pion transfers momentum to the pion field, but that the interactions between that field and the nucleon are such as to enhance emission of pions in the "resonant" state. The implied separation into pion-nucleon and pion-pion interactions is, of course, somewhat artificial, since the two should be considered as different aspects of the same phenomenon in a consistent theory.

VII. COMPARISON WITH OTHER EXPERIMENTS

As mentioned in Sec. III, our best estimate for the total $\pi^- - p$ cross section at our energy agrees well with the counter determination of 34±3 millibarns.[4] Counter measurements had given an indication that small-angle scatterings were frequent, which is well confirmed by our angular distribution for diffraction scattering.

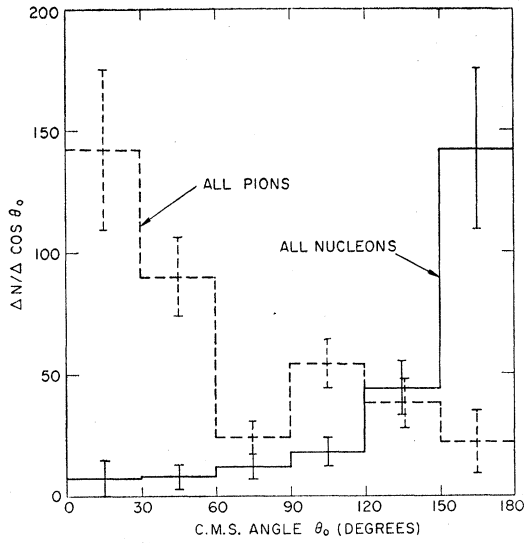

FIG. 11. Center-of-mass differential angular distributions for all pions and nucleons from $(p-0)$ and $(n+-)$ events, based on same events as Figs. 5–10.

Emulsion results have also shown that most elastic scatterings occur at small angles.[5]

In making a detailed comparison of our results with the emulsion data of Crussard, Walker, and Koshiba,[5] it is important to note that about half of the emulsion events were considered to involve interactions with protons bound in nuclei. Such interactions would not be expected to be exactly the same as those of free protons. Emulsions provide better information on density of ionization than our diffusion chambers. On the other hand, no information on the sign of electric charge can be obtained. Information on outgoing pion energies is more often available in the cloud chamber data so that our analysis includes an attempt to identify events

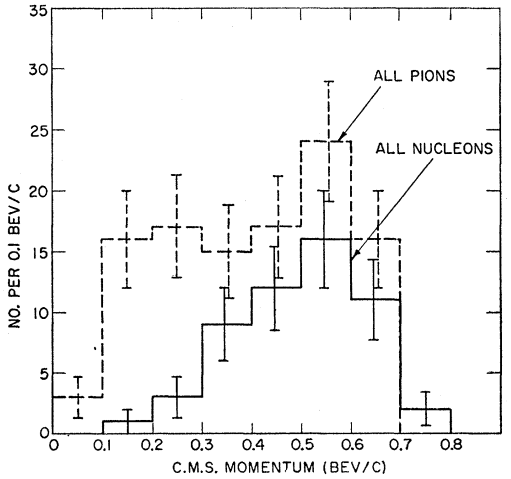

FIG. 12. Center-of-mass momentum distributions for all pions and nucleons from $(p-0)$ and $(n+-)$ events, based on same events as Figs. 5–10.

involving double pion production while this process was assumed to be negligible in the emulsion experiment.

The results are in good general agreement, considering the differences in procedure. Our data show a somewhat higher fraction of elastic events, 162/470 instead of 16/68, probably because they are more difficult to recognize in the emulsion events. In each case the number of $(p-+-)$ is small. In each case the ratio of $(p-0)$ to $(n+-)$ is about unity within statistics: 20/30 for cloud chamber, 31/20 for emulsion. In both experiments the inelastic scatterings show a marked tendency for the nucleons to be emitted backwards in c.m. system. The conclusions concerning angular distribution of pions are somewhat different in that the emulsion data seem to show a very definite low energy backwards group and high energy forwards group in c.m. system, which were interpreted as being pions emitted from an excited nucleon and scattered incident pions, respectively. In the cloud chamber data most pions tend to go forwards, and the apparent backwards group of π^+ is probably due to a selection bias. Attempts to calculate Q values for the hypothetical excited nucleon were inconclusive in both cases.

VIII. CONCLUSIONS

The results show that inelastic collisions in which secondary pions are produced are common at an energy of 1.37 Bev (65 percent of all interactions resulting in charged particles). There are some cases in which two secondary pions are produced (an estimated 15 percent of the inelastic collisions resulting in charged particles). The frequencies of events with different pion multiplicities are not well determined because of the difficulty of analyzing cases with poor momentum measurements, but seem to be very roughly consistent with the predictions of the Fermi statistical theory (Table IV). Elastic scatterings (35 percent of all interactions) occur mainly at angles $<30°$ in the laboratory system, and are mainly a shadow scattering phenomenon. This indicates that the region in which the incoming pion interacts has a radius of about 1.2×10^{-13} cm and is somewhat transparent, a conclusion which is inconsistent with the statistical model's basic assumption of very strong interaction. An alternate interpretation fitting the observed cross sections $\sigma_{el}=10$ mb and $\sigma_{inel}=24$ mb, and the observed large angle elastic scattering, would indicate the existence of a region near the center where the interaction is very strong ($\lambda\approx0$) and an outside region where the interactions becomes quite weak ($\lambda\approx5\times10^{-13}$ cm).

Angular correlations of pions suggest that pion-pion interactions may play a role in the interactions studied. The momentum spectra of the pions seem to show low and high groups which may be due to the $T=J=\frac{3}{2}$ "resonant" state. No definite conclusions are possible on these last points, and they are presented mainly as questions to be answered by future experiments.

We are indebted to the Cosmotron staff for providing us with very reliable operation of the machine, and to the other members of the cloud chamber group for their effective help in operating the cloud chamber equipment. M. R. Burns and F. S. Keene have aided us considerably by scanning most of the photographs.